SHORT COMMUNICATION

Multiparametric mapping in post-mortem perinatal MRI: a feasibility study

[1]AMY R MCDOWELL, PhD, [2]SUSAN C SHELMERDINE, [1,3]SARA LORIO, PhD, [1,4]WENDY NORMAN, [1,4]ROD JONES, [1,3]DAVID W CARMICHAEL, PhD and [2,4]OWEN J ARTHURS, PhD

[1]UCL Great Ormond Street Institute of Child Health, London, UK
[2]RadiologyGreat Ormond Street Hospital NHS Foundation Trust, London, UK
[3]Wellcome EPSRC Centre for Medical EngineeringKCL, London, UK
[4]NIHR UCL GOS Institute of Child Health Biomedical Research Centre, London, UK

Address correspondence to: Dr Amy R McDowell
E-mail: *a.mcdowell@ucl.ac.uk*

Objectives: To demonstrate feasibility of a 3 T multiparametric mapping (MPM) quantitative pipeline for perinatal post-mortem MR (PMMR) imaging.

Methods: Whole body quantitative PMMR imaging was acquired in four cases, mean gestational age 34 weeks, range (29–38 weeks) on a 3 T Siemens Prisma scanner. A multicontrast protocol yielded proton density, T_1 and magnetic transfer (MT) weighted multi-echo images obtained from variable flip angle (FA) 3D fast low angle single-shot (FLASH) acquisitions, radiofrequency transmit field map and one B_0 field map alongside four MT weighted acquisitions with saturation pulses of 180, 220, 260 and 300 degrees were acquired, all at 1 mm isotropic resolution.

Results: Whole body MPM was achievable in all four foetuses, with R_1, R_2*, PD and MT maps reconstructed from a single protocol. Multiparametric maps were of high quality and show good tissue contrast, especially the MT maps.

Conclusion: MPM is a feasible technique in a perinatal post-mortem setting, which may allow quantification of post-mortem change, prior to being evaluated in a clinical setting.

Advances in knowledge: We have shown that the MPM sequence is feasible in PMMR imaging and shown the potential of MT imaging in this setting.

INTRODUCTION

Paediatric autopsy rates have declined over recent decades, leading to increased usage of post-mortem magnetic resonance imaging (PMMR) for non-invasive assessment.[1] Whilst its usage in the perinatal population has been reported to have a high diagnostic accuracy rate,[2] there is still room for further improvement particularly when differentiating pathologies *vs* those of post-mortem changes to the body. Improvements over the current sequences used for PMMR may be helpful

Ideally, a PMMR protocol should comprise of three-dimensional (3D), isovolumetric, whole-body imaging, with coverage of all the major organs within a single imaging volume. However, these have adapted from those of live neonatal imaging where certain constraints such as patient movement and the avoidance of general anaesthesia where possible, play a role. As such, these current post-mortem whole-body sequences are split into several volumes—usually of low resolution and suboptimal T_1 and T_2 weighting across the body in a single acquisition.[3,4]

A recent study suggested that a semi-quantitative magnetisation transfer (MT) ratio may be a better post-mortem measure of cardiac abnormalities[5] than conventional $T_{1/2}$ imaging, and that MT imaging was sensitive to brain development due to its ability to delineate myelination.[6] Within the post-mortem imaging literature however, there are limited published data on its potential clinical impact.

Quantitative MPM mapping comprises of three series of low flip-angle spoiled gradient-echo images acquired in a single protocol and was developed to provide absolute MR parameter measures that are comparable across sites and at different time points.[7] We have developed a multiparametric mapping (MPM) pipeline for post-mortem foetal whole-body imaging, that can generate 3D proton density (PD), longitudinal relaxation rate R_1 (1/T_1), effective transverse relaxation rate R_2* (1/T_2*) and magnetisation transfer (MT) saturation saturation maps using variable flip angles. Here, we perform an optimisation of the sequence for usage in perinatal PMMR imaging and present the results of a pilot study in a preliminary set of test cases.

METHODS AND MATERIALS

Ethics

Ethical approval was granted for this prospective, single centre study (REC 09/H0713/2). Parental written consent for post-mortem imaging was obtained in each case.

Case selection

Consecutive unselected perinatal deaths of age above 21 weeks of gestation, and all but severe maceration states were included, referred to our institution Great Ormond Street Hospital, for specialist perinatal autopsy opinion. Bodies were stored in the mortuary at 4°C and PMMR was performed outside of clinical hours to ensure minimal disturbance to imaging services. Cases were transferred directly from the mortuary to scanner, with foetus positioned in a head coil in the supine position, and wrapped with insulating material to aid temperature stability.

MPM optimisation

The MPM sequence had previously been developed for use in the adult in-vivo brain which has an average T_1 of 1000 ms.[8] It is well known that the foetal brain has a much higher T_1 value with values above 2000 ms.[9] Therefore, T_1 and T_2 maps of the foetal brain were estimated using a different acquisition protocol to inform the parameters used in the MPM sequence.

A first set of 10 post-mortem foetuses were imaged at 3 T on the Siemens Prisma using a 64-channel head coil. Inversion recovery turbo spin echo images were acquired with inversion times of 200, 600, 1000, 1500 and 2000 ms for T_1 map calculation (TE 13 ms, TR 12000 ms, pixel size 0.7×0.7 mm, slice thickness 2 mm),

and a Carr-Purcell-Meiboom-Gill sequence for T_2 map calculation (32-echo train length, TE 13.4 ms, TR 5000 ms, 0.9×0.9 mm).

T_1 maps were calculated using code by Barral et al,[10] T_2 maps with imageJ (odd echoes were discarded for the calculation). Voxels of interest (VOIs) were identified for white matter (WM) and grey matter (GM) in the frontal, temporal, occipital, sensory/motor, basal ganglia and in the pons (T_1 only). The T_1 and T_2 was calculated in WM and GM in each foetus by averaging the values across all VOIs.

MPM acquisition

Whole-body (vertex to mid-thigh) quantitative MPM images of a second set of four foetuses were performed with a 3 T Siemens Prisma. PD, T_1 and MT weighted (respectively PDW, T_1W, MTW) images were acquired with spatial resolution of 1 mm^3. PDW and T_1W multiecho 3D fast low-angle shot (FLASH) acquisitions[7,8] were acquired, alongside four MTW acquisitions with saturation pulses of 180°, 220°, 260° and 300° (Table 1).

An RF transmit field map using 3D echoplanar imaging (EPI) spin echo (SE) and stimulated echo (STE) images was used to correct B_1 field inhomogeneities, and one B_0 field map was acquired using a two-dimensional double-echo FLASH sequence to correct the RF transmit field maps for geometric distortion and off-resonance effects.[11] An external syringe containing 0.09 mg/ml Gadolinium was placed by the head for calibration of the PD maps as detailed in Lorio et al.[12] Details of MT measurement can be found in Helms et al.[13] Conventional clinical 3D

Table 1. Sequence parameters used for the multiparametric mapping protocol

Parameter	Acquisition parameters
Scanner type	Siemens Prisma
Field strength	3 T
Gradient	80 mT/m
	200 T/m/s magnetic field gradients
Coil	64-channel head coil
Acquisition	Whole-body
MPM Sequence	
PD mapping	Sagittal; TR/FA 24.5 ms/6°; matrix 240×256
T1 mapping	Sagittal; TR/FA 24.5 ms/21°; eight equidistant echo times (TEs between 2.34–18.72 ms); matrix 240×256
MT mapping	Sagittal; TR/FA 24.5/6° with six equidistant TEs between 2.3 and 14.04 ms; matrix 240×256
MT pulse FA	180°, 220°, 260° and 300°
Specific absorption rate	1.01, 1.47, 2.02, and 2.66 W/Kg for 180°, 220°, 260° and 300° MT pulses respectively
Voxel size	1 mm isotropic for PDW, T_1W and MTW
B1 mapping	4 mm isotropic; TR 250 ms; TEs of 19.55 and 39.1 ms; FAs of the SE/STE refocusing pulses were decreased from 230°/115°–130°/65° in steps of 10°/5°; matrix 48×64
B0 mapping	64 axial slices; slice thickness 2 mm; matrix 64×64; FA 90°; TR 1020 ms; TE1/TE2 10/12
Times of Acquisition (minutes)	T_1W 9:21; PDW 9:21; MTW 9:21; B_1 1:30; B_0 2:38; Total 32:20

FA, flip angle; MPM, multiparametric mapping; MT, magnetic transfer; PD, proton density; TE, echo time; TR, repetition time.

T_2 weighted images were acquired according to our normal protocol[3]; MPM images were not used for clinical diagnoses in this feasibility study.

Image interpretation

Maps were calculated using in-house software in SPM (http://www.fil.ion.ucl.ac.uk/spm) based on Weiskopf et al[7] with further developments to improve R_2* map quality and enable PD mapping without anatomical priors.[12] VOIs were drawn manually using MIPAV by a single reader (SCS), a specialised in paediatric radiology (9 years of general radiology training, 4 years of paediatric and post-mortem imaging experience). These were placed in multiple brain and body areas (Frontal Lobe WM, Frontal Lobe GM, Temporal Lobe WM, Temporal Lobe GM, Occipital Lobe WM, Occipital Lobe GM, Basal Ganglia, Pons, Cerebellum, Right Lung, Left Lung, Myocardium, Right Lobe Liver, Left lobe liver, Spleen, Right Renal Cortex, Left renal cortex, Right Psoas and Left Psoas as described in previous publications[14,15]) and saved as a VOI data set and overlaid across all quantitative maps. Further statistical or quantitative image analysis was not undertaken in this feasibility study.

RESULTS

MPM optimisation

Conventional T_1 and T_2 maps were acquired in 10 foetuses with a mean gestational age of 31 weeks, range 23–39 weeks. WM T_1 mean/range values were 1073/763–1242 ms, for T2 194.5/159–233 ms; and GM T_1 mean/range values were 1006/773–1283 ms and T_2 182.7/122–271 ms. The adult GM/WM T_1 range (for which the MPM sequence is optimised[8]) is between 748 and 1258 ms, and therefore it was reasonable to implement the MPM sequence unchanged for PMMR. The lower values of T_1 and T_2 obtained compared to in-vivo values is likely due to post-mortem changes and lower temperature of the foetuses at scanning.

MPM acquisition

We acquired PMMR imaging in four foetuses, mean gestational age 34 weeks, range 29–38 weeks at 3 T. These were two males, two females, with mean birthweight 1900 g, range 940–3100 g. Two cases were normal at imaging and autopsy with no final diagnosis; one had subtle cortical malformation with mild ventriculomegaly, and the other agenesis of the corpus callosum with complex congenital heart disease. MPM was feasible in all four of our foetal cases; an example is shown in Figure 1 comparing T_2 weighted imaging with MPM maps at 3 T. All MPM maps of the four foetuses are shown in Figure 2.

The corrected PD maps showed little contrast with little difference in the free-water proton density values within the soft tissues post-mortem (shown in Figure 3A). Figure 2 shows PD maps of all four cases. All cases showed poor contrast in the brain. However, panels i and iii demonstrated higher detail in the liver and heart.

The R1 map images showed high contrast in the brain and body organs with clear delineation of all of the abdominal organs and the heart. An interesting decrease in T_1 was observed at the bottom of the abdominal space surrounding the internal organs and in the wall of the abdomen, which may be due to blood or protein-rich ascites. This size of this artefact was variable and extended the range of R_1 values in the abdomen (Figure 3B).

R_2* maps had high contrast within the abdomen, but poorer in the brain. They also suffered from high signal artefacts around the skin surface, and inside the body such as the pericardiac sac and sinuses. These were likely to be susceptibility-related artefacts as they are adjacent to regions containing air or gas, and may have affected values in these areas (Figure 3C).

The semi-quantitative MT saturation maps were found to have higher MT signal values at higher MT pulse angles as expected. Ratios of MT signal value in the brain (GM/WM) and the body (myocardium/liver) were taken for the four MT saturation pulse flip angles (Table 2). There was no significant increase in contrast ratio between tissues with MT saturation pulse angle. To benefit from the higher signal values, the MT map produced using a flip angle of 300 degrees was used for all further analysis. Overall, the MT maps appeared to have the best signal and contrast between organs of all the quantitative maps. Figure 3D shows the average MT values from all cases.

Figure 1. Example of quantitative MPM maps. The left-hand panel shows a conventional coronal T_2 weighted 2D image in a 31 week gestation post-mortem foetus. The right-hand four panels show quantitative maps produced using the MPM sequence and processing in the same foetus. 2D, two-dimensional; MPM, multiparametric mapping.
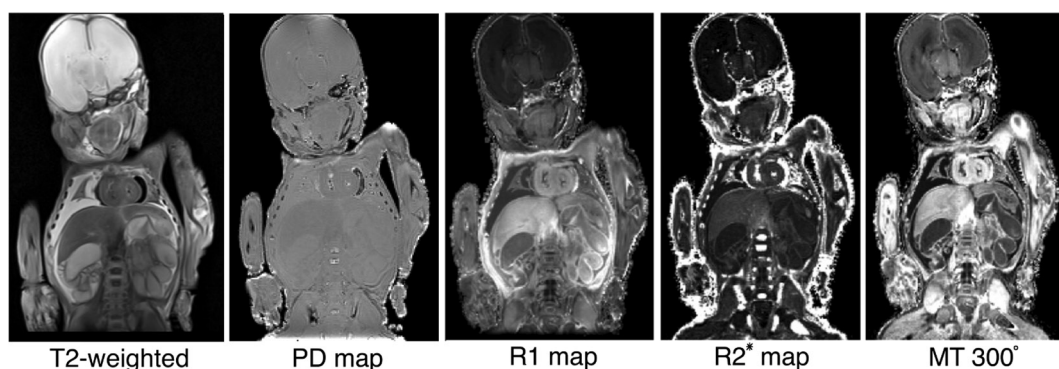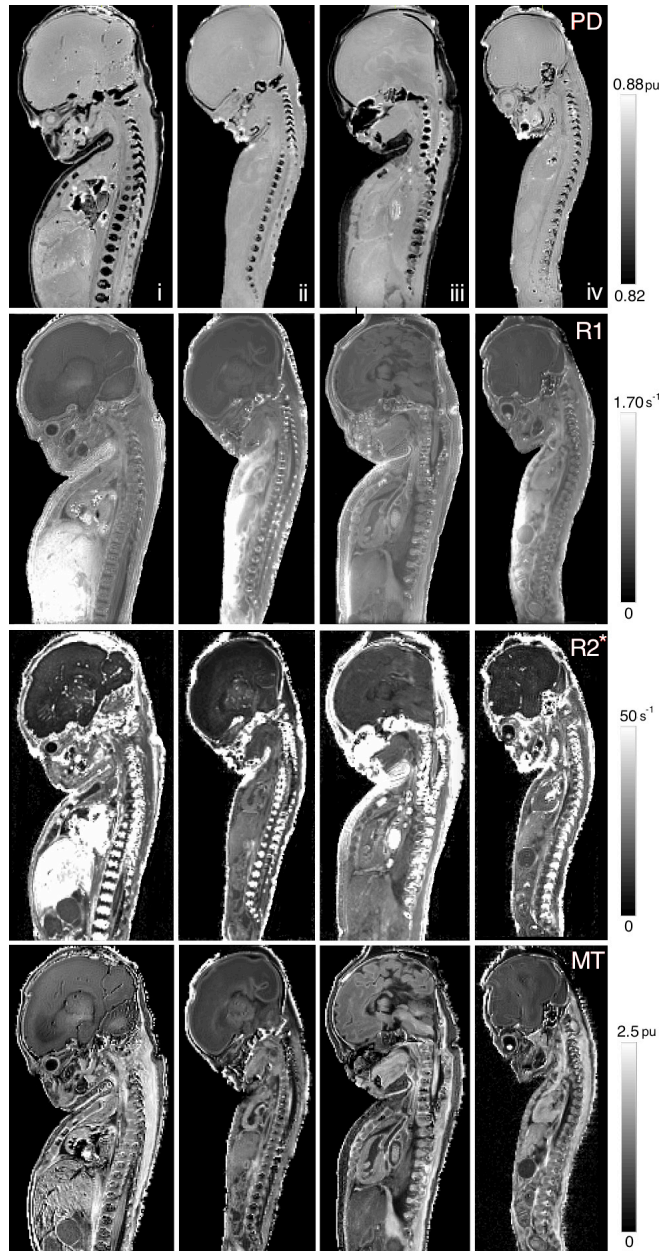

T2-weighted   PD map   R1 map   R2* map   MT 300°

Figure 2. Sagittal MPM maps of all four cases at 3 T. PD, R_1, R_2^*, and MT maps are shown for case i (3100 g at 37 weeks gestation), ii (940 g at 29 weeks gestation), iii (2500 g at 37 weeks gestation), and iv, (1180 g at 31 weeks gestation). MPM, multiparametric mapping; MT, magnetic transfer; PD, proton density

typical weighted MR image signal intensity (*e.g.* B_1 transmit and receive field variations as well as B_0 field variations) are removed to derive quantitative maps that facilitate visual and quantitative comparison because map values are only related to the underlying tissue properties without additional sequence and hardware-related effects.

MPM would be of particular use in a post-mortem setting, where the range of absolute tissue parameter values encountered is wide, both between and within cases. Some of the challenges of in-vivo clinical studies using MPM (*e.g.* patient motion, image alignment) are absent in the post-mortem setting making implementation straightforward. The quantification of MR imaging parameters, such as T_1 and T_2, is preferable to relying on qualitatively examining their effect on image contrast. These quantitative measurements should not vary across sequences or different scanner manufacturers, and should facilitate longitudinal studies and across-site comparisons.
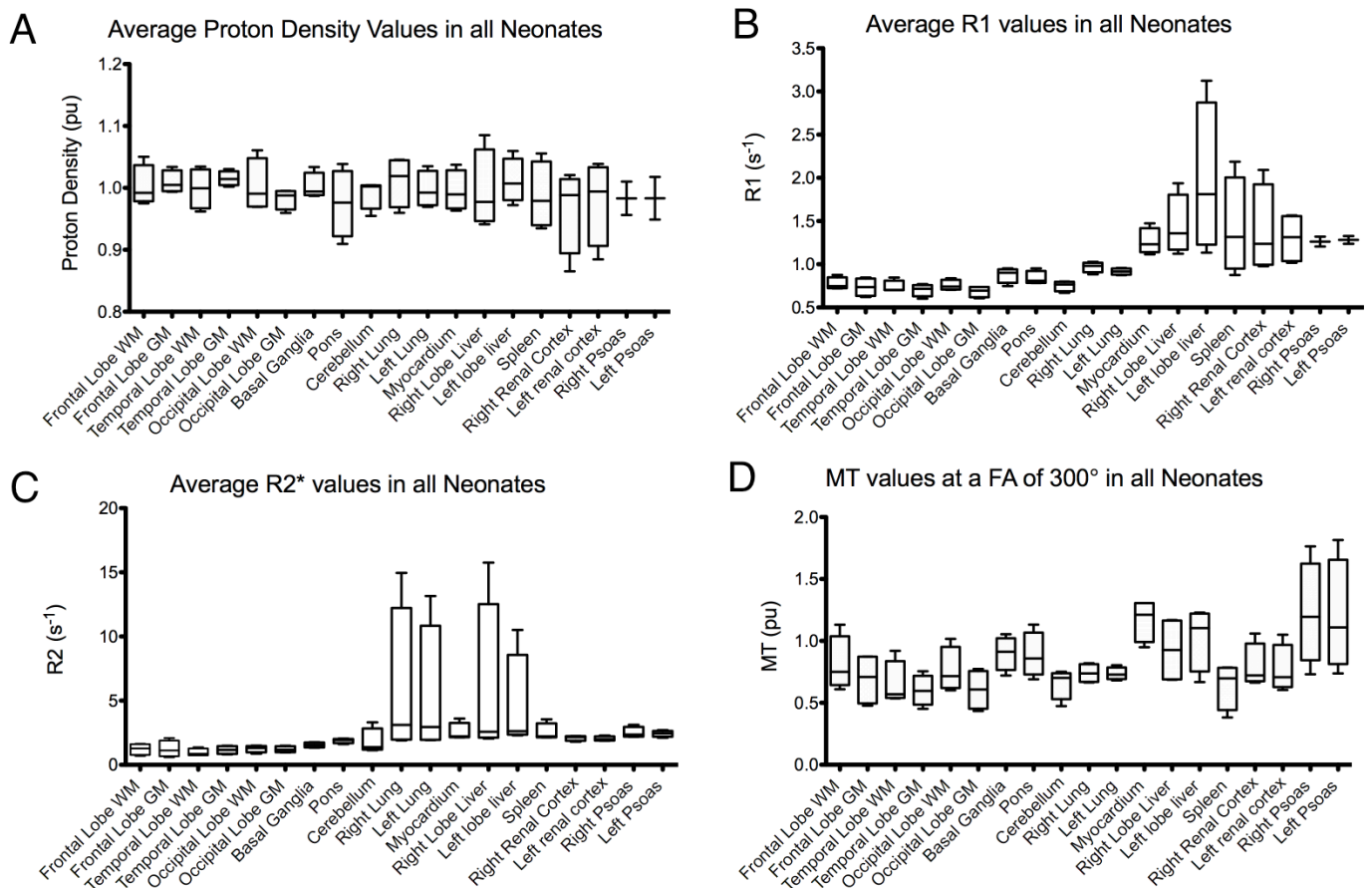
When comparing PD maps in Figure 2, we noticed better contrast in the two larger foetuses in the group (panels i and iii), who weighed 3100 g and 2500 g at 37 weeks gestation. Larger cases may have better soft tissue preservation post-mortem, maintaining organ structure and corresponding PD contrast. In the two smaller cases (ii, 940 g at 29 weeks gestation; and iv, 1180 g at 31 weeks gestation) cell breakdown and maceration is likely to have contributed to an almost uniform free PD in the soft tissues. Although PD maps may not yield diagnostic organ imaging in our cohort, quantitative values may still represent useful data on degree of maceration or time since death, although this would need to be tested in a larger cohort.

Both PD and R_2^* maps had limitations: the PD demonstrated poor contrast, whereas the strong B0 inhomogeneity due to susceptibility changes at air/tissue interfaces made R_2^* mapping challenging. The application of quantitative magnetic susceptibility (QSM) mapping could remove these effects,[16] although this would require optimisation. However, we speculate that the quantitative data generated in these maps could still be useful when used in conjunction with other measures.

Semi-quantitative MT maps showed increased signal with an increased MT saturation pulse, but no difference in contrast in the major organs. There was high variability in the MT values within and between subjects. MT changes are related to the formation of myelinated structures and recently, there has been interest in using MT values for the evaluation of pathological changes in skeletal muscle.[17] In the post-mortem case, the variability might be due to differing factors such as time from death, but would require further investigation in a larger cohort. The brain, myocardium and liver showed highly variable MT values and could be tested against histological markers also in a larger cohort for validation.

We found that MT maps were of good quality, and had the potential to provide extra information to the autopsy. We suggest that a standard MT imaging sequence could be a valuable addition to standard PMMR protocols even where there are not the resources

DISCUSSION

Multiparametric maps were feasible for foetal PMMR. This is the first reported use of magnetisation transfer maps in this setting to our knowledge. This sequence allowed the acquisition of high-resolution imaging of the whole-body to provide multiple quantitative maps (PD, R_1, R_2^*, MT) from a single protocol.

Multiparametric mapping has several different advantages, including quantification of data and high scanning efficiency. Crucially, the correction of the other factors that influence

Figure 3. Box and whisker plots of average quantitative MPM values in all foetuses. Whiskers are maximum and minimum values. PD values are shown in panel A; R_1 values (panel B) show high variability in the abdominal organs of liver, spleen and kidneys due to the artefacts seen in Figure 2; R_2* values (panel C) have high variability in lung and liver also due to artefacts; MT values (panel D) are shown for a MT flip angle of 300°. MPM, multiparametric mapping; MT, magnetic transfer; PD, proton density.

A — Average Proton Density Values in all Neonates

B — Average R1 values in all Neonates

C — Average R2* values in all Neonates

D — MT values at a FA of 300° in all Neonates

to add a full MPM imaging and reconstruction protocol, although commercial versions are becoming more widely available.

CONCLUSION

We have demonstrated MPM feasibility in a whole-body perinatal post-mortem setting. Quantitative maps, particularly R_1 and MT saturation maps, showed high contrast. This protocol may be useful in future post-mortem evaluation and be amenable to more advanced computational analysis in a larger cohort.

ACKNOWLEDGMENT

AUTHORSHIP

All authors have made substantial contributions to 1) substantial contributions to conception and design, or acquisition of data, or analysis and interpretation of data; 2) drafting the article or revising it critically for important intellectual content; and 3) final approval of the version to be published.

ETHICS

Ethical approval was granted for this prospective, single centre study (REC 09/H0713/2). Parental written consent for post-mortem imaging was obtained in each case.

Table 2. MT contrast assessment in the post-mortem foetal brain (GM/WM) and body (myocardium/liver) with differing MT saturation pulse flip angle

MT flip angle	180°	220°	260°	300°
GM/WM ratio	1.51	1.54	1.54	1.56
Myocardium/Liver ratio	1.14	1.17	1.16	1.17

GM, grey matter; MT, magnetic transfer; WM, white matter.

REFERENCES

1. Nicholl RM, Balasubramaniam VP, Urquhart DS, Sellathurai N, Rutherford MA. Postmortem brain MRI with selective tissue biopsy as an adjunct to autopsy following neonatal encephalopathy. *Eur J Paediatr Neurol* 2007; **11**: 167–74. doi: https://doi.org/10.1016/j.ejpn.2006.12.004

2. Arthurs OJ, Taylor AM, Sebire NJ, Indications SNJ. Indications, advantages and limitations of perinatal postmortem imaging in clinical practice. *Pediatr Radiol* 2015; **45**: 491–500. doi: https://doi.org/10.1007/s00247-014-3165-z

3. Norman W, Jawad N, Jones R, Taylor AM, Arthurs OJ. Perinatal and paediatric post-mortem magnetic resonance imaging (PMMR): sequences and technique. *Br J Radiol* 2016; **89**: 20151028. doi: https://doi.org/10.1259/bjr.20151028

4. Shelmerdine SC, Hutchinson JC, Sebire NJ, Jacques TS, Arthurs OJ. resonance P-mortemmagnetic PMMR) imaging of the brain in fetuses and children with histopathological correlation. *Clinical radiology* 2017; **72**: 1025–37.

5. Crooijmans HJA, Ruder TD, Zech W-D, Somaini S, Scheffler K, Thali MJ, et al. Cardiovascular magnetization transfer ratio imaging compared with histology: a postmortem study. *J Magn Reson Imaging* 2014; **40**: 915–9. doi: https://doi.org/10.1002/jmri.24460

6. Korostyshevskaya AM, Prihod'ko IY, Savelov AA, Yarnykh VL. Direct comparison between apparent diffusion coefficient and macromolecular proton fraction as quantitative biomarkers of the human fetal brain maturation. *J Magn Reson Imaging* 2019; **50**: 52–61. doi: https://doi.org/10.1002/jmri.26635

7. Weiskopf N, Suckling J, Williams G, Correia MM, Inkster B, Tait R, et al. Quantitative multi-parameter mapping of R1, PD(*), MT, and R2(*) at 3T: a multi-center validation. *Front Neurosci* 2013; **7**: 95. doi: https://doi.org/10.3389/fnins.2013.00095

8. Helms G, Dathe H, Dechent P. Quantitative flash MRI at 3T using a rational approximation of the Ernst equation. *Magn Reson Med* 2008; **59**: 667–72. doi: https://doi.org/10.1002/mrm.21542

9. Schneider J, Kober T, Bickle Graz M, Meuli R, Hüppi PS, Hagmann P, et al. Evolution of T1 relaxation, ADC, and fractional anisotropy during early brain maturation: a serial imaging study on preterm infants. *AJNR Am J Neuroradiol* 2016; **37**: 155–62. doi: https://doi.org/10.3174/ajnr.A4510

10. Barral JK, Gudmundson E, Stikov N, Etezadi-Amoli M, Stoica P, Nishimura DG. A robust methodology for in vivo T1 mapping. *Magn Reson Med* 2010; **64**: 1057–67. doi: https://doi.org/10.1002/mrm.22497

11. Lutti A, Hutton C, Finsterbusch J, Helms G, Weiskopf N. Optimization and validation of methods for mapping of the radiofrequency transmit field at 3T. *Magn Reson Med* 2010; **64**: 229–38. doi: https://doi.org/10.1002/mrm.22421

12. Lorio S, Tierney TM, McDowell A, Arthurs OJ, Lutti A, Weiskopf N, et al. Flexible proton density (PD) mapping using multi-contrast variable FLIP angle (VFA) data. *Neuroimage* 2019; **186**: 464–75. doi: https://doi.org/10.1016/j.neuroimage.2018.11.023

13. Helms G, Dathe H, Dechent P. Modeling the influence of TR and excitation FLIP angle on the magnetization transfer ratio (mtr) in human brain obtained from 3D spoiled gradient echo MRI. *Magn Reson Med* 2010; **64**: 177–85. doi: https://doi.org/10.1002/mrm.22379

14. Arthurs OJ, Rega A, Guimiot F, Belarbi N, Rosenblatt J, Biran V, et al. Diffusion-Weighted magnetic resonance imaging of the fetal brain in intrauterine growth restriction. *Ultrasound Obstet Gynecol* 2017; **50**: 79–87. doi: https://doi.org/10.1002/uog.17318

15. McDowell AR, Shelmerdine SC, Carmichael DW, Arthurs OJ. High resolution isotropic diffusion imaging in post-mortem neonates: a feasibility study. *Br J Radiol* 2018; **91**: 20180319. doi: https://doi.org/10.1259/bjr.20180319

16. Wang Y, Liu T, mapping Q. QSM): decoding MRI data for a tissue magnetic biomarker. *Magnetic resonance in medicine* 2015; **73**: 82–101.

17. Sinclair CDJ, Samson RS, Thomas DL, Weiskopf N, Lutti A, Thornton JS, et al. Quantitative magnetization transfer in in vivo healthy human skeletal muscle at 3 T. *Magn Reson Med* 2010; **64**: 1739–48. doi: https://doi.org/10.1002/mrm.22562